Journal of Advanced Zoology

ISSN: 0253-7214

*Volume **44** Issue 5 **Year 2023** Page 1460-**1473***

Molecular Docking And Visualization Of Selected Phytochemicals For Using Software Autodock Vina And Pymol

Haseera. N[1], Baskaran. K[2*], Shalet Varghese[1], Nirmala Devi.N[1]

[1,2]Department of Biochemistry, Sree Narayana Guru College, Coimbatore, Tamilnadu, India.*

***Corresponding Author:** Dr. K. Baskaran*
MSC, M.Phil., Ph.D. Assistant Professor, Department of Biochemistry, Sree Narayana Gure College, Coimbatore-641105, Tamil Nādu, India, E-mail: baskar.bio86@gmail.com, Cell number: 91+8760302579

Article History:

Received: 10 Nov 2023
Revised: 30 Nov 2023
Accepted: 10 Dec 2023

Abstract

The accurate prediction of protein−ligand binding affinity is a central challenge in computational chemistry and insilico drug discovery. The free energy perturbation (FEP) method based on molecular dynamics (MD) simulation provides accurate results only if a reliable structure is available via high-resolution X-ray crystallography. To overcome the limitation, we propose a sequential prediction protocol using generalized replica exchange with solute tempering AutoDock Vina and PyMOL. At first, ligand binding poses are predicted using PyMOL, which weakens protein−ligand interactions at high temperatures to multiple binding poses. To avoid ligand dissociation at high temperatures, a flat-bottom restraint potential centered on the binding site is applied in the simulation. The binding affinity of the most reliable pose is then calculated using FEP. The protocol is applied to the bindings of ten ligands to FK506 binding proteins AutoDock Vina showing the excellent agreement between the calculated and experimental binding affinities. The present protocol, which is referred to as the AutoDock Vina and PyMOL method, would help to predict the binding affinities without high-resolution structural information on the ligand-bound state.

Keywords: Molecular dynamics, AutoDock Vina and PyMOL

INTRODUCTION

The accurate prediction of protein−ligand binding affinity is one of the key challenges in computational chemistry and Insilco drug design because of its potential to reduce the cost and time for drug development. X-ray crystal structures of target protein−ligand complexes give structural information on the binding sites and poses, which is essential to predict the binding affinities. Even when the binding site is known, there may exist multiple binding poses in the site. Since the binding affinity depends severely on the binding pose, the determination of reliable poses is a prerequisite for high-precision drug design. To date, a variety of computational methods have been proposed for pose prediction (Lim, et al., 2016; Gallicchio, et al., 2010).

Protein−ligand docking methods predict multiple binding poses and calculate their affinities. Since the docking methods are fast and computationally efficient, they are widely used to virtually screen potential drug candidates (Araki, et al., 2016; Jones, et al., 1997; Morris, et al., 1998). However, protein flexibility is not sufficiently considered in most of the docking simulations, while ligand bindings often couple with protein conformational changes. Many different types of functions have been developed, although they often simplify the protein−ligand interactions based on the shape complementarity and treat solvation effects implicitly, missing physical components including entropy contributions from solvent molecules and proteins. Docking methods are less accurate in ranking the predicted poses and sometimes overlook plausible binding poses (Friesner, et al., 2004; Halgren, et al., 2004; Friesner, et al., 2006).

The AutoDock Vina v.1.1.2 was used to simulate the docking of the 64 compounds which was obtained in the GC analysis, and the docking data with the highest binding score were displayed to examine the molecular interactions (Trott, et al., 2009). The CASTp v.3.0 program was used to define and measure the volume of the active catalytic site of the target protein. The amino acids which may participate in the docking in the active site were predicted, and the affinity grid maps were identified using the AutoGrid tool of the AutoDock Tools package (Allen, et al., 2015; Warren, et al., 2006).

The global search exhaustiveness was set at 8 and a total of 9 binding modes were present. The weights and terms scoring function was set to default parameters. Furthermore, AutoDock Vina uses a gradient algorithm search method to predict the binding scores and modes of ligands in the active receptor sites. Visualization of the docking was done with the help of PyMOL v.2.5.2 (Mobley, et al., 2014; Aldeghi, et al., 2015; Gaieb, et al., 2019).

MATERIAL AND METHODS

Protein/macromolecule

The 3-dimensional structure was extracted in PDB format from the RCSB PDB data repository. PDB id given to the structure and primarily structure is a homodimer having two A chains composed of 306 amino acids and N3 molecule acting as its inhibitor.

Ligands

A total of 21 bioactive compounds from five different plants including Allium cepa L. Elettaria cardamomum maton, Curcuma longa, Zingiber officinale, Allium sativum *ginseng* were selected as ligands and structures were obtained from PubChem databank in.sdf format. For the docking purpose, all the ligands were converted into.pdb file format using Biovia Discovery Studio Visualizer

Molecular docking

To obtain protein–ligand docked complex Autodock 4.2 was utilized. The downloaded structure and each ligand was optimized prior to docking. From the protein 3D structure, water molecules and the inhibitor N3 molecule were removed. Addition of polar hydrogen bonds, Kollman charges and Gasteiger charges summed up the protein and ligand optimization. A grid box of 60 × 60 × 60 was prepared around the binding site of the protein with 0.375 Å spacing. Genetic algorithm was set as the search parameter and output was handled in Lamarckian GA run and docking log file (DLG) were obtained for further analysis of binding energy. The analysis of DLG file revealed a total of 10 conformations for each ligand. The conformation with highest negative binding energy was selected and docked complex was converted to a 2D structure to examine the interactions formed at binding site with ligand.

RESULT AND DISCUSSION

ADME analysis

Lipinski's rule of five was applied to estimate the drug likeliness of the all selected 38 candidates. This comparative method helps us to rule out few compounds according to their physiochemical properties. Compounds violating two or more parameters were out listed and rest of the compounds were considered to be ligands for the docking study. Out of 58 phytochemicals, , remaining 21 compounds were subjected to docking studies (Table 1).

Table 1. Showing details of the ligands selected for analysis

Sl. No	Ligand Code	Chemical Compound	Chemical Formula	% Probabili	Molecular Weight	PubChem ID	CAS No

				ty	(g/mol)		
1	Lig1	Cyclic octa-atomic sulfur	S8	98.61	256.5	66348	10544-50-0
2	Lig2	Dimethyl trisulfide	C2H6S3	98.48	126.3	19310	3658-80-8
3	Lig3	Trisulfide, dipropyl	C6H14S3	94.87	182.4	22383	6028-61-1
4	Lig4	Trisulfide, methyl propyl	C4H10S3	94.4	154.3	5319765	17619-36-2
5	Lig5	Tetrasulfide, dipropyl	C6H14S4	92.76	214.4	104285	52687-98-6
6	Lig6	Disulfide, methyl propyl	C4H10S2	78.21	122.3	16592	2179-60-4
7	Lig7	Tetrasulfide, dimethyl	C2H6S4	77.89	158.3	79828	5756-24-1
8	Lig8	Disulfide, dipropyl	C6H14S2	51.42	150.3	12377	629-19-6
9	Lig9	5-Methyl-1,2,3,4-tetrathiane	C3H6S4	42.32	170.3	5319787	116664-30-3
10	Lig10	(E)-1-(Prop-1-en-1-yl)-3-propyltrisulfane	C6H12S3	29.69	180.4	5352693	23838-27-9
11	Lig11	Disulfide, 1-methylethyl propyl	C6H14S2	29.61	150.3	118529	33672-51-4
12	Lig12	3,5-diethyl-1,2,4-Trithiolane	C6H12S3	-	180.4	520895	54644-28-9
13	Lig13	1-Propenylpropyldisulfide	C6H12S2	-	148.3	5352908	23838-20-2
14	Lig14	N,N-Dimethylthioformamide	C3H7NS	-	89.16	69794	758-16-7
15	Lig15	1-Methoxycyclohexene	C7H12O	-	112.17	70264	931-57-7
16	Lig16	1,1,2-Trifluoro-1,3-butadiene	C4H3F3	-	108.06	109645	565-65-1
17	Lig17	2-methyl-3-butyn-2-ol	C5H8O	-	84.12	8258	115-19-5
18	Lig18	Methylglycinate	C3H7NO2	-	89.09	69221	616-34-2
19	Lig19	Methanesulfonylazide	CH3N3O2S	-	121.12	556271	1516-70-7
20	Lig20	Di-1-propenyltrisulfide	C6H10S3	-	178.3	5352793	-
21	Lig21	Trans-3,5-diethyl-1,2,4-trithiolane	C6H12S3	-	180.4	6432398	38348-26-4

Molecular docking

All the filtered ligands from the ADME analysis were subjected to molecular docking analysis. Molecular docking is an essential computational tool in the drug discovery domain. It is done to further select the potential compounds and study the bond formation in the protein–ligand complex at the binding site. Figure 1,2,3 represents all 6 residues namely: Pro142(A), Met27(A), Gly5(A), Thr30(A), Ala26(A), Phe25(A) & Ala26(A), Met 27(A), Ser 141(A), Thr140(A), Pro142(A), Phe25(A) and Pro142(A), Ser141(A), Met27(A), Gly5(A), Thr140(A), Phe25(A) which are present in at the active site of the M-pro protein. N3 (native

inhibitor) was taken as a control and comparative study of the docking results of all 31 ligands (Table 1,2,3) with the control revealed that four compounds having better binding energy as compared with the binding energy of N3 (-2.9,-2.3,-3.4 kcal/mol).

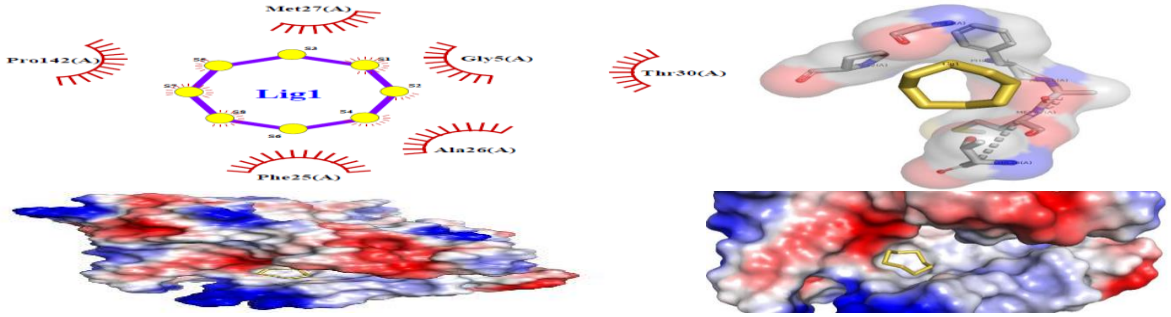

Fig 1 Visualisation of docking interaction and 3D H-bonding, docked pose of lig1

Ligand Code	Binding Affinity (kcal/mol)	No. of H-bonding	H-Bond forming Amino Acids	H-Bond Distance: Donor – Acceptor (A)	Hydrophobic Interaction forming Amino Acids	No. of hydro-phobic bond
Lig1	-2.9				Pro142(A), Met27(A), Gly5(A), Thr30(A), Ala26(A), Phe25(A)	6

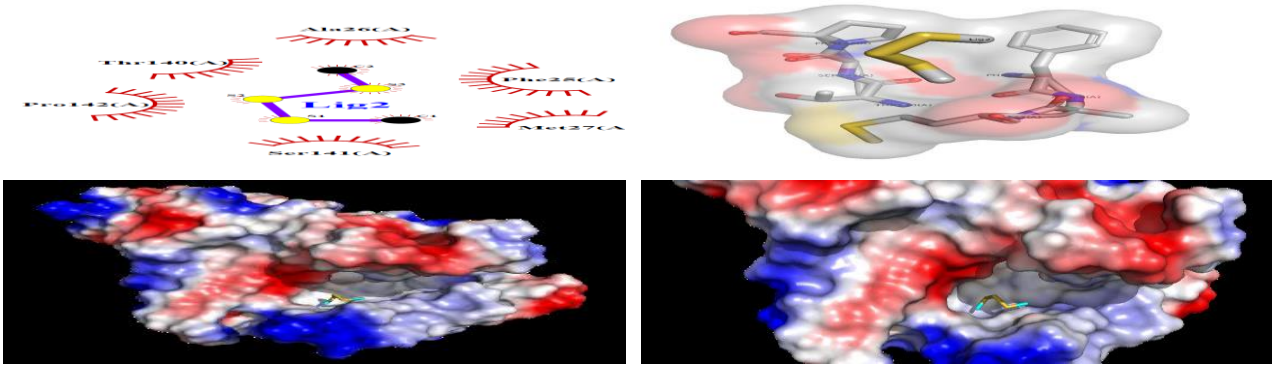

Fig 2 Visualisation of docking interaction and 3D H-bonding, docked pose of lig2

Ligand Code	Binding Affinity (kcal/mol)	No. of H-bonding	H-Bond forming Amino Acids	H-Bond Distance: Donor – Acceptor (A)	Hydrophobic Interaction forming Amino Acids	No. of hydro-phobic bond
Lig2	-2.3				Ala26(A), Met 27(A), Ser 141(A), Thr140(A), Pro142(A), Phe25(A)	6

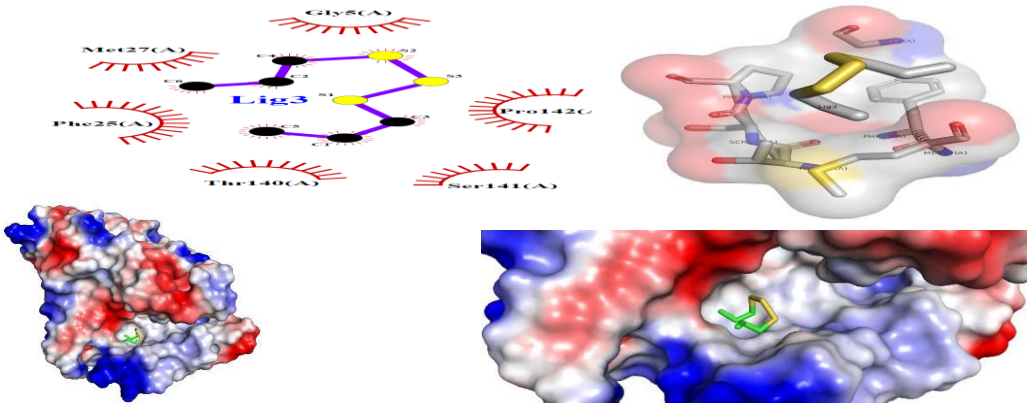

Fig 3 Visualisation of docking interaction and 3D H-bonding, docked pose of lig3

Ligand Code	Binding Affinity (kcal/mol)	No. of H-bonding	H-Bond forming Amino Acids	H-Bond Distance: Donor – Acceptor (A)	Hydrophobic Interaction forming Amino Acids	No. of hydro-phobic bond
Lig3	-3.4				Pro142(A), Ser141(A), Met27(A), Gly5(A), Thr140(A), Phe25(A)	6

Among the 7 conformation of Nimbin, − 8.66 kcal/ mol was the least binding energy obtained. Five different types of interaction were observed including van der waals, H-bond, alkyl, pi-alkyl and carbon hydrogen bond (Fig. 4,5,6). Phe25(A), Gly5(A), Met27(A), Ser141(A), Thr140(A),Pro142(A), Met145(A) forming the conventional H-bond while Gly5(A), Phe25(A), Met27(A), Pro142(A), Thr140(A),Ser141(A), Met145(A) were engaged with a pi-alkyl and alkyl bond respectively. Gly5(A), Phe25(A), Met27(A), Ala26(A), Pro142(A), Thr30(A were interacting with the ligand using carbon hydrogen bond and remaining residues weakly interact with the ligand via van der waals bond formation.

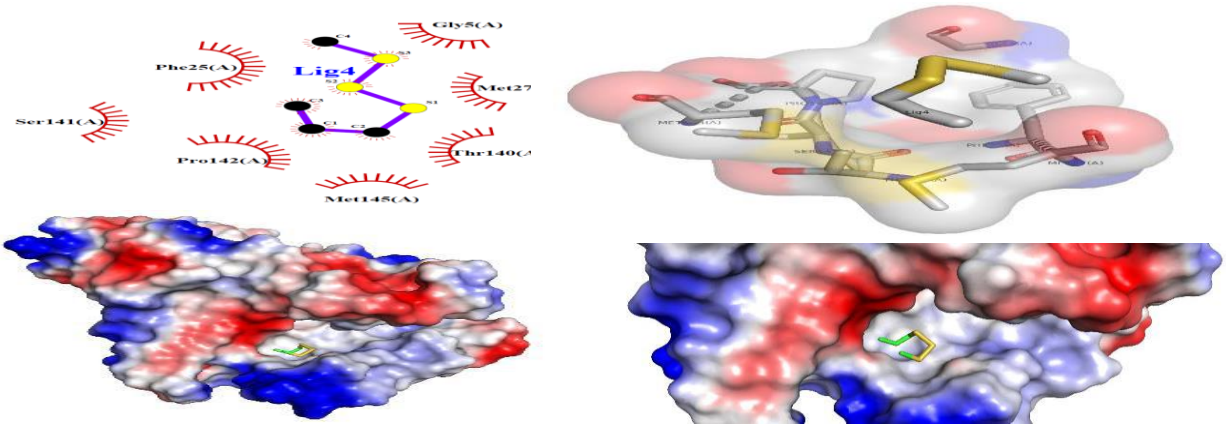

Fig 4 Visualisation of docking interaction and 3D H-bonding, docked pose of lig4

Ligand Code	Binding Affinity (kcal/mol)	No. of H-bonding	H-Bond forming Amino Acids	H-Bond Distance: Donor – Acceptor (A)	Hydrophobic Interaction forming Amino Acids	No. of hydro-phobic bond
Lig4	-3				Phe25(A), Gly5(A), Met27(A), Ser141(A), Thr140(A),Pro142(A), Met145(A)	7

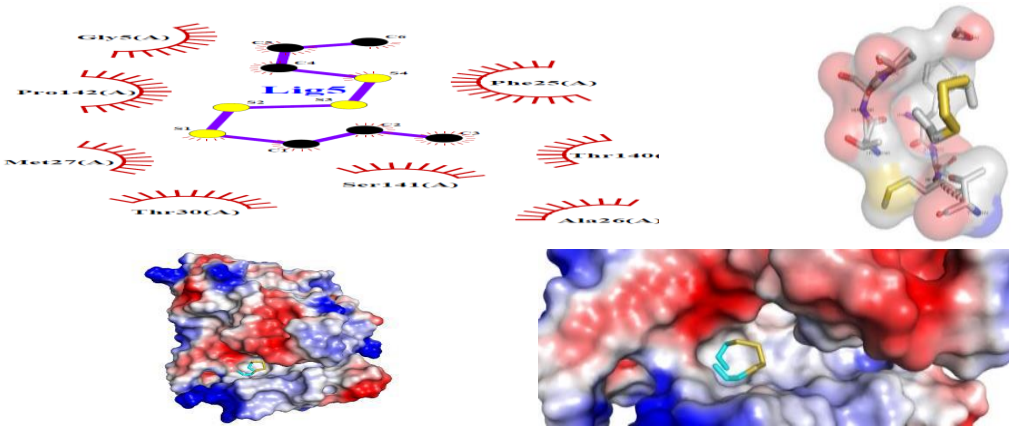

Fig 5 Visualisation of docking interaction and 3D H-bonding, docked pose of lig5

Ligand Code	Binding Affinity (kcal/mol)	No. of H-bonding	H-Bond forming Amino Acids	H-Bond Distance: Donor – Acceptor (A)	Hydrophobic Interaction forming Amino Acids	No. of hydro-phobic bond
Lig5	-3.4				Gly5(A), Phe25(A), Met27(A), Pro142(A), Thr140(A),Ser141(A), Met145(A)	7

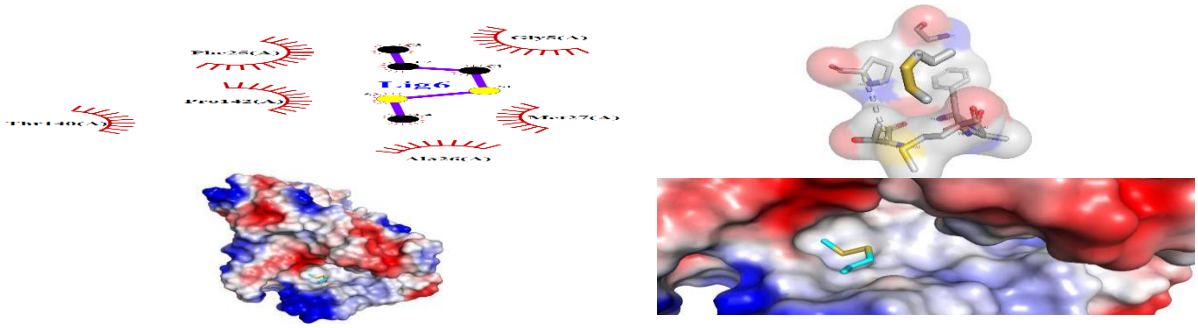

Fig 6 Visualisation of docking interaction and 3D H-bonding, docked pose of lig6

Ligand Code	Binding Affinity (kcal/mol)	No. of H-bonding	H-Bond forming Amino Acids	H-Bond Distance: Donor – Acceptor (A)	Hydrophobic Interaction forming Amino Acids	No. of hydro-phobic bond
Lig6	-3				Gly5(A), Phe25(A), Met27(A), Ala26(A), Pro142(A), Thr30(A)	6

Gedunin-Mpro complex (Fig. 7,8,9,10) the minimum binding energy. A sum total of 7 types of bond formation was observed. Phe25(A), Met27(A), Ala26(A), Pro142(A), Thr30(A), Met145(A) formed convention H-bond, pi-anion bond and carbon hydrogen bond with gedunin. Thr30(A), Phe25(A), Ser141(A),Thr140(A), Gly5(A), Pro142(A), Ala26(A), Met27(A), Met145(A) forms a pi-sigma as well as pi-alkyl bonds while Thr30(A), Phe25(A), Ser141(A),Thr140(A), Pro142(A), Ala26(A), Met27(A) formed alkyl bonds. Ser141(A), Pro142(A), Thr140(A) Phe25(A), Gly5(A), Thr30(A), Met145(A) both formed carbon hydrogen bond. His143 contributed to stabilization by forming an additional pi-alkyl bond remaining all the residues were attracted to the ligand by van der waals bond. Epoxyazadiradione was the other compound with binding energy greater than of control.

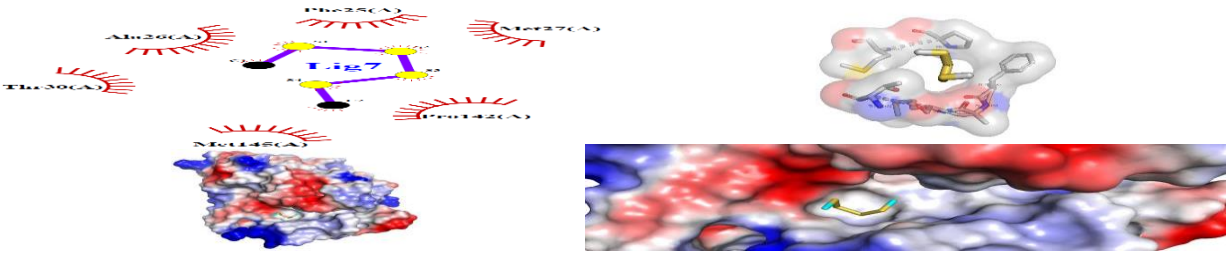

Fig 7 Visualisation of docking interaction and 3D H-bonding, docked pose of lig

Ligand Code	Binding Affinity (kcal/mol)	No. of H-bonding	H-Bond forming Amino Acids	H-Bond Distance: Donor – Acceptor (A)	Hydrophobic Interaction forming Amino Acids	No. of hydro-phobic bond
Lig7	-2.4				Phe25(A), Met27(A), Ala26(A), Pro142(A), Thr30(A), Met145(A)	6

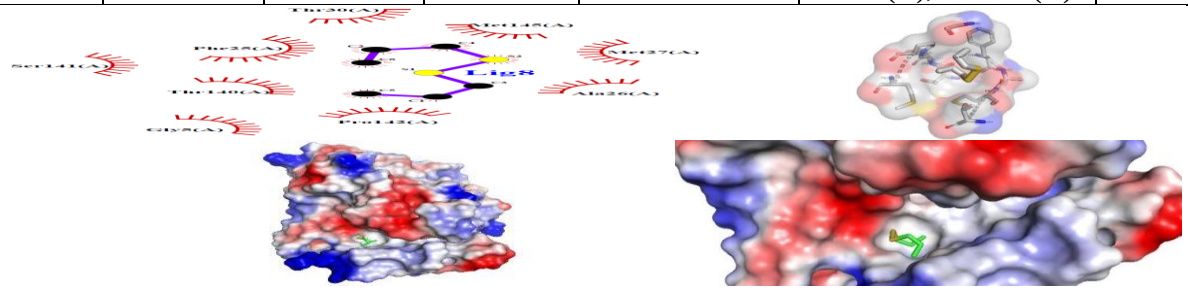

Fig 8 Visualisation of docking interaction and 3D H-bonding, docked pose of lig8

Ligand Code	Binding Affinity (kcal/mol)	No. of H-bonding	H-Bond forming Amino Acids	H-Bond Distance: Donor – Acceptor (A)	Hydrophobic Interaction forming Amino Acids	No. of hydro-phobic bond
Lig8	-3.4				Thr30(A), Phe25(A), Ser141(A),Thr140(A), Gly5(A), Pro142(A), Ala26(A), Met27(A), Met145(A)	9

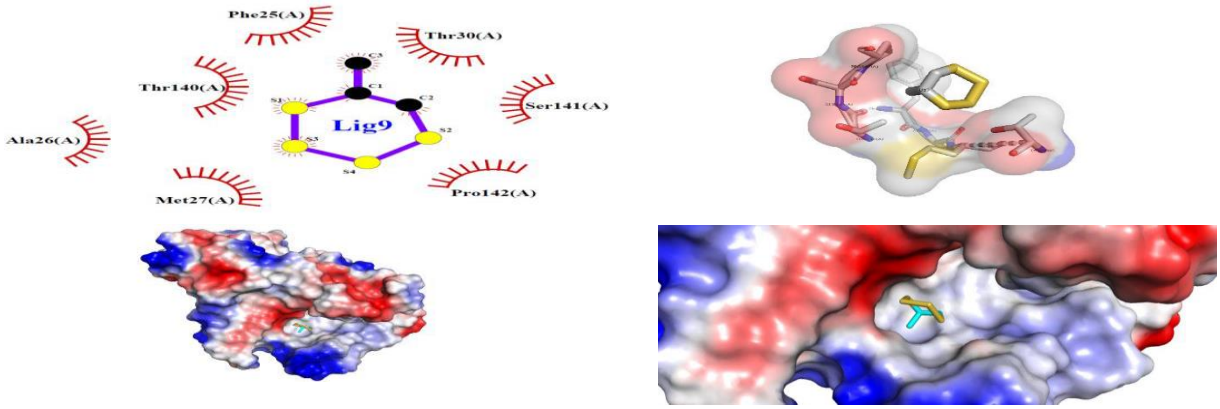

Fig 9 Visualisation of docking interaction and 3D H-bonding, docked pose of lig9

Ligand Code	Binding Affinity (kcal/mol)	No. of H-bonding	H-Bond forming Amino Acids	H-Bond Distance: Donor – Acceptor (A)	Hydrophobic Interaction forming Amino Acids	No. of hydro-phobic bond
Lig9	-3.3				Thr30(A), Phe25(A), Ser141(A),Thr140(A),	7

					Pro142(A), Ala26(A), Met27(A)	

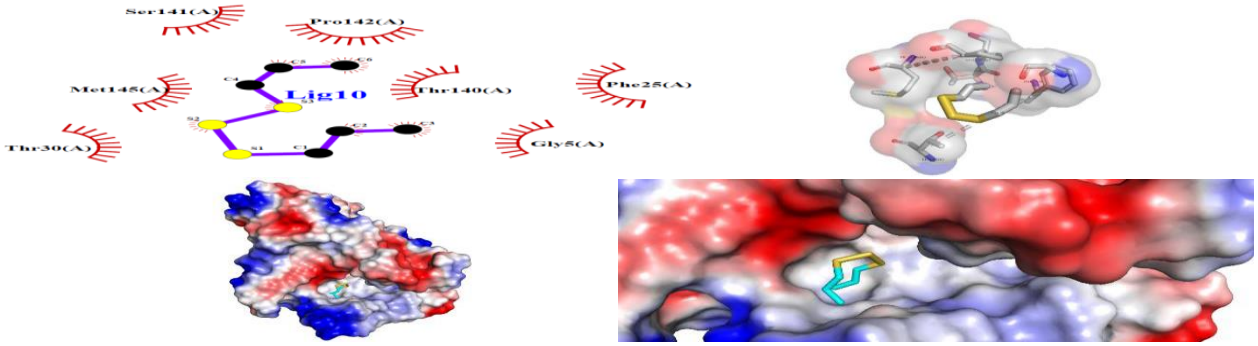

Fig 10 Visualisation of docking interaction and 3D H-bonding, docked pose of lig10

Ligand Code	Binding Affinity (kcal/mol)	No. of H-bonding	H-Bond forming Amino Acids	H-Bond Distance: Donor – Acceptor (A)	Hydrophobic Interaction forming Amino Acids	No. of hydro-phobic bond
Lig10	-3.4				Ser141(A), Pro142(A), Thr140(A) Phe25(A), Gly5(A), Thr30(A), Met145(A)	7

Four types of interaction can be observed. Along with numerous residues involved in weak van der waals interaction, Pro142(A),Ser141(A), Thr30(A), Met27(A), Gly5(A), Thr140(A), Ala26(A), Phe25(A) forms H-bond. Pro142(A),Ser141(A), Met27(A), Gly5(A), Thr140(A), Phe25(A), Thr30(A), Ala26(A) formed alkyl bonds and Thr25 forms a carbon hydrogen bond (Fig. 11,12).

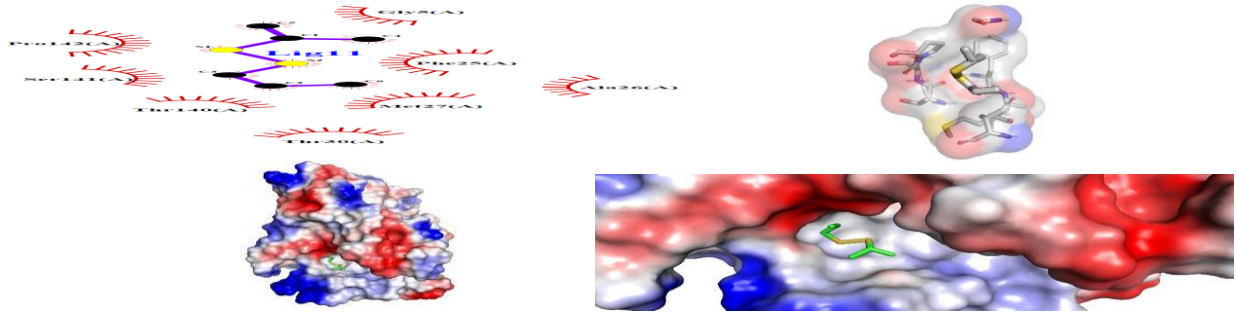

Fig 11 Visualisation of docking interaction and 3D H-bonding, docked pose of lig11

Ligand Code	Binding Affinity (kcal/mol)	No. of H-bonding	H-Bond forming Amino Acids	H-Bond Distance: Donor – Acceptor (A)	Hydrophobic Interaction forming Amino Acids	No. of hydro-phobic bond
Lig11	-3.5				Pro142(A),Ser141(A), Thr30(A), Met27(A), Gly5(A), Thr140(A), Ala26(A), Phe25(A)	8

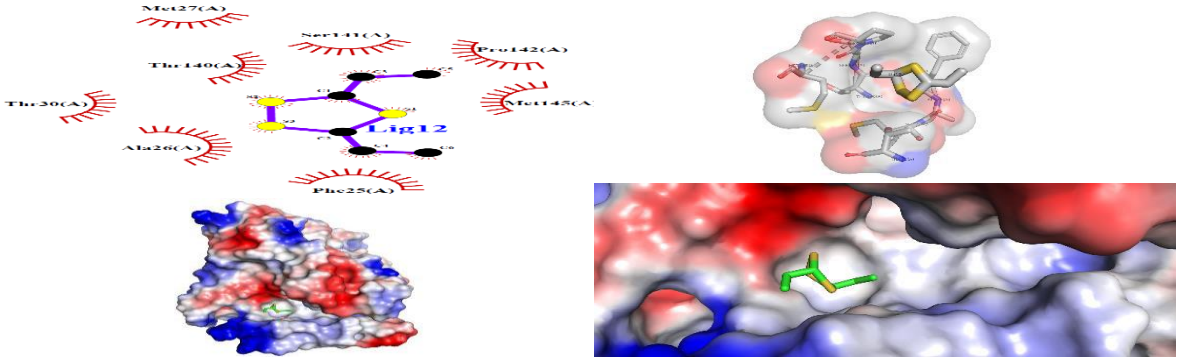

Fig 12 Visualisation of docking interaction and 3D H-bonding, docked pose of lig12

Ligand Code	Binding Affinity (kcal/mol)	No. of H-bonding	H-Bond forming Amino Acids	H-Bond Distance: Donor – Acceptor (A)	Hydrophobic Interaction forming Amino Acids	No. of hydro-phobic bond
Lig12	-3.8				Pro142(A),Ser141(A), Met27(A), Gly5(A), Thr140(A), Phe25(A), Thr30(A), Ala26(A)	8

Ginsenosides-Mpro complex showed the minimum binding energy of -4.4kcal/mol among all the conformations and ligands. A total of six different type of stabilizing interactions were observed. A conventional H-bond formation was done by Pro142(A), Ser141(A), Met27(A), Gly5(A), Thr140(A), Phe25(A) residues Pro142(A),Ser141(A), Thr30(A), Met27(A), Gly5(A), Thr140(A), Ala26(A), Phe25(A) pi-sigma and pi-alkyl with 3 atoms of the ligand. Ala38(A), Val101(A), Ser106(A), Lys42(A), Lys41(A), Phe110(A) and Val101(A),Ser106(A), Ala38(A), Phe110(A) helped stabilizing complex via alkyl bond formation. Nine more residues can be observed around the ginsenosides interacting via van der waals forces (Fig. 13,14,15.16).

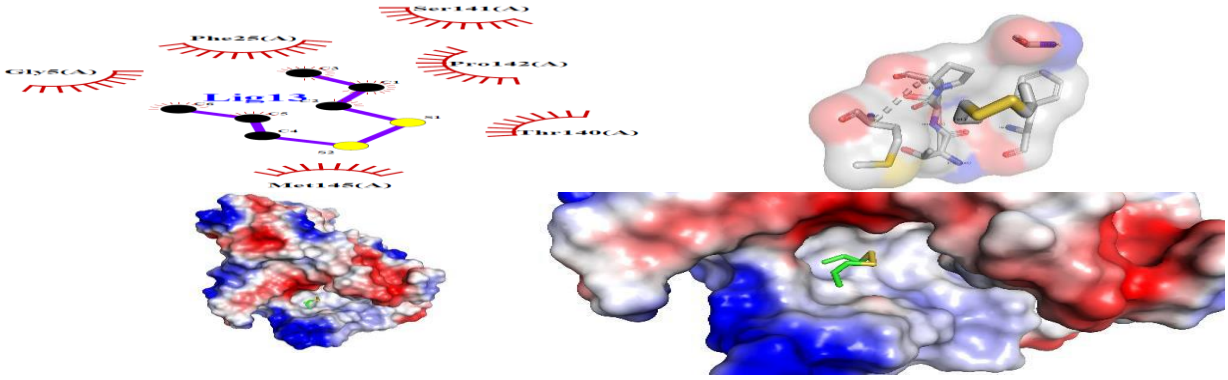

Fig 13 Visualisation of docking interaction and 3D H-bonding, docked pose of lig1 3

Ligand Code	Binding Affinity (kcal/mol)	No. of H-bonding	H-Bond forming Amino Acids	H-Bond Distance: Donor – Acceptor (A)	Hydrophobic Interaction forming Amino Acids	No. of hydro-phobic bond
Lig13	-3.4				Pro142(A), Ser141(A), Met27(A), Gly5(A), Thr140(A), Phe25(A)	6

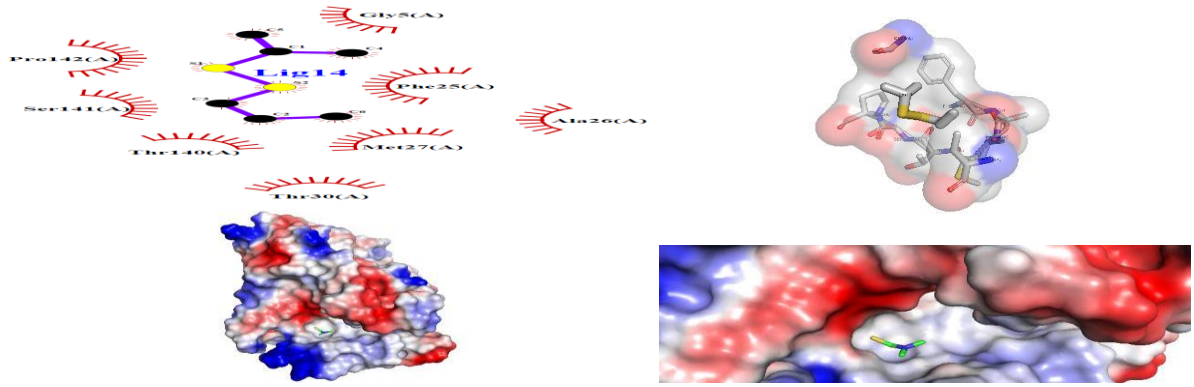

Fig 14 Visualisation of docking interaction and 3D H-bonding, docked pose of lig1

Ligand Code	Binding Affinity (kcal/mol)	No. of H-bonding	H-Bond forming Amino Acids	H-Bond Distance: Donor – Acceptor (A)	Hydrophobic Interaction forming Amino Acids	No. of hydro-phobic bond
Lig14	-2.4				Pro142(A),Ser141(A), Thr30(A), Met27(A), Gly5(A), Thr140(A), Ala26(A), Phe25(A)	8

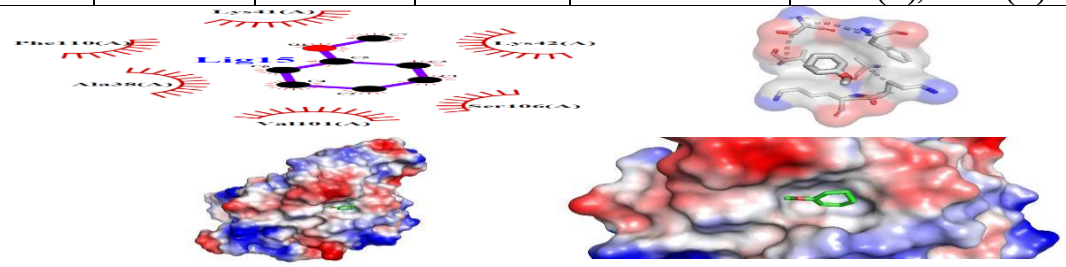

Fig 15 Visualisation of docking interaction and 3D H-bonding, docked pose of lig15

Ligand Code	Binding Affinity (kcal/mol)	No. of H-bonding	H-Bond forming Amino Acids	H-Bond Distance: Donor – Acceptor (A)	Hydrophobic Interaction forming Amino Acids	No. of hydro-phobic bond
Lig15	-4.4				Ala38(A), Val101(A), Ser106(A), Lys42(A), Lys41(A), Phe110(A)	6

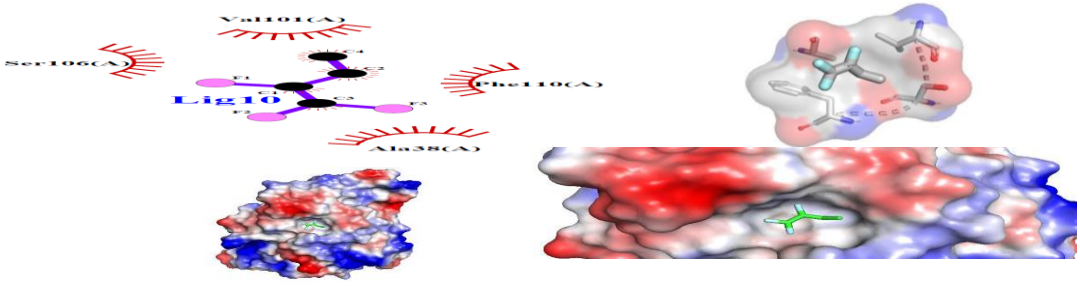

Fig 16 Visualisation of docking interaction and 3D H-bonding, docked pose of lig16

Ligand Code	Binding Affinity (kcal/mol)	No. of H-bonding	H-Bond forming Amino Acids	H-Bond Distance: Donor – Acceptor (A)	Hydrophobic Interaction forming Amino Acids	No. of hydro-phobic bond
Lig16	-4				Val101(A),Ser106(A), Ala38(A), Phe110(A)	4

Among the 7 conformation of Nimbin, -3.9 kcal/ mol was the least binding energy obtained. Five different types of interaction were observed including van der waals, H-bond, alkyl, pi-alkyl and carbon hydrogen bond (Fig. 17,18,19,20,21). Ser141(A), Phe25(A), Met145(A), Ala26(A), Pro142(A) forming the conventional H-bond Thr140(A) while Asn129(A), Tyr64(A) H-bond Ser29(A) Ser29(A) Asn91(A) Asn91(A) Ser89(A) Ser89(A) were engaged with a pi-alkyl and alkyl bond respectively. Tyr64(A), Glu125(A) H-bond Ser29(A) Asn129(A) Asn63(A) Asn91(A) Ser89(A) were interacting with the ligand using carbon hydrogen bond and remaining residues weakly interact with the ligand via van der waals bond formation. Phe25(A), Gly5(A), Ser141(A), Thr140(A), Pro142(A), Thr30(A) and Gly5(A), Phe25(A), Pro142(A), Thr30(A), Met145(A).

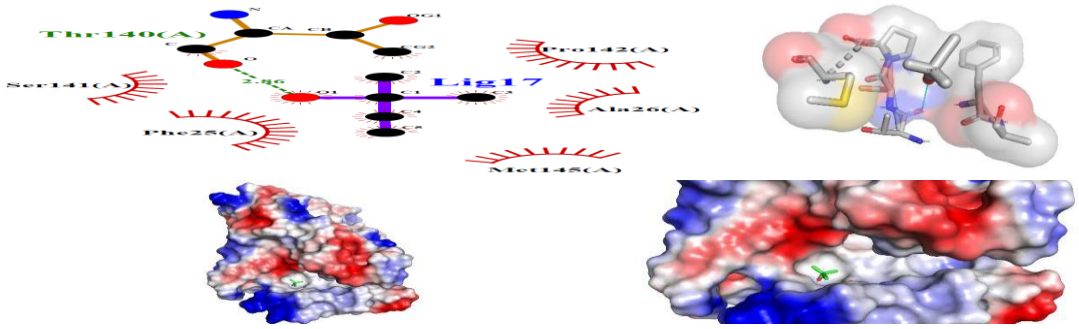

Fig 17 Visualisation of docking interaction and 3D H-bonding, docked pose of lig17

Ligand Code	Binding Affinity (kcal/mol)	No. of H-bonding	H-Bond forming Amino Acids	H-Bond Distance: Donor – Acceptor (A)	Hydrophobic Interaction forming Amino Acids	No. of hydro-phobic bond
Lig17	-3.9	1	Thr140(A)	2.86	Ser141(A), Phe25(A), Met145(A), Ala26(A), Pro142(A)	5

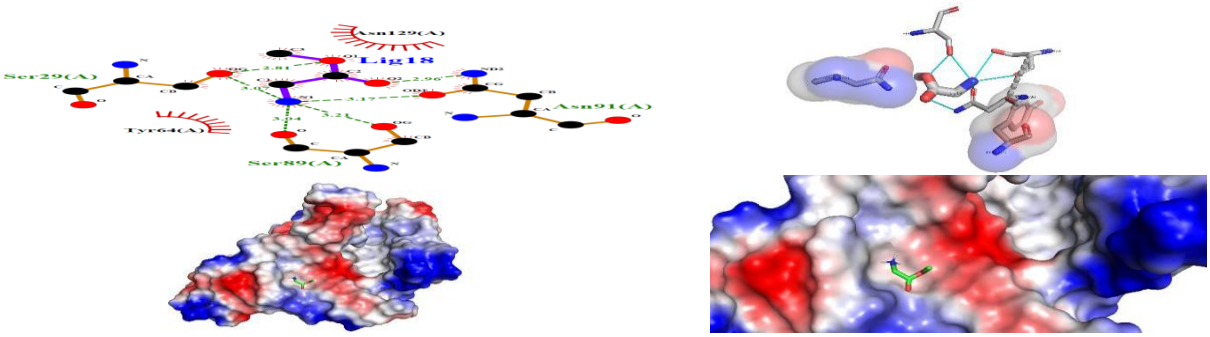

Fig 18 Visualisation of docking interaction and 3D H-bonding, docked pose of lig18

Ligand Code	Binding Affinity (kcal/mol)	No. of H-bonding	H-Bond forming Amino Acids	H-Bond Distance:Donor – Acceptor (A)	Hydrophobic Interactionforming Amino Acids	No. of hydro-phobic bond
Lig18	-3.5	6	Ser29(A) Ser29(A) Asn91(A) Asn91(A) Ser89(A) Ser89(A)	2.81 3.07 2.96 3.17 3.21 3.04	Asn129(A), Tyr64(A)	2

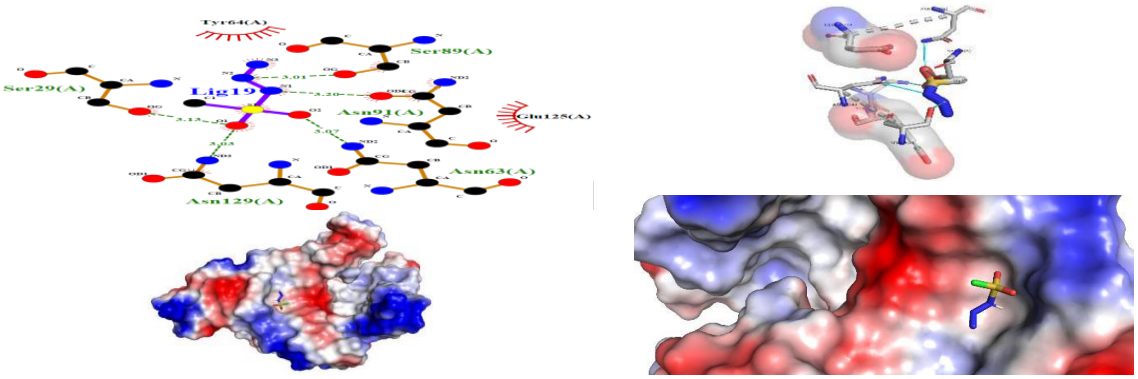

Fig 19 Visualisation of docking interaction and 3D H-bonding, docked pose of lig19

Ligand Code	Binding Affinity (kcal/mol)	No. of H-bonding	H-Bond forming Amino Acids	H-Bond Distance: Donor – Acceptor (A)	Hydrophobic Interaction forming Amino Acids	No. of hydro-phobic bond
Lig19	-4.2	5	Ser29(A) Asn129(A) Asn63(A) Asn91(A) Ser89(A)	3.13 3.03 3.07 3.20 3.01	Tyr64(A), Glu125(A)	2

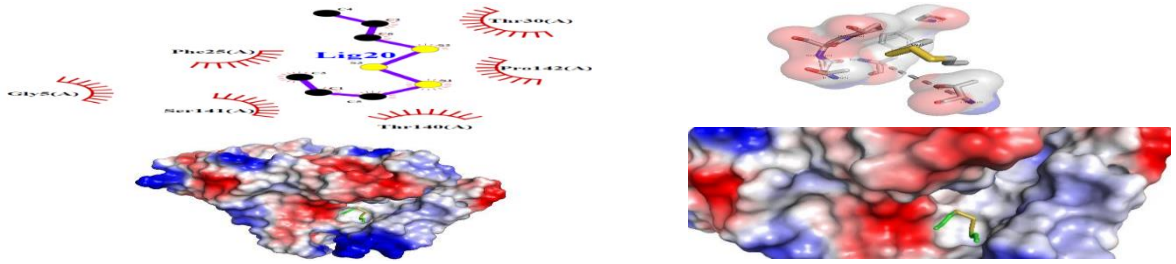

Fig 20 Visualisation of docking interaction and 3D H-bonding, docked pose of lig20

Ligand Code	Binding Affinity (kcal/mol)	No. of H-bonding	H-Bond forming Amino Acids	H-Bond Distance: Donor – Acceptor (A)	Hydrophobic Interaction forming Amino Acids	No. of hydro-phobic bond
Lig20	-3.4				Phe25(A), Gly5(A), Ser141(A), Thr140(A), Pro142(A), Thr30(A)	6

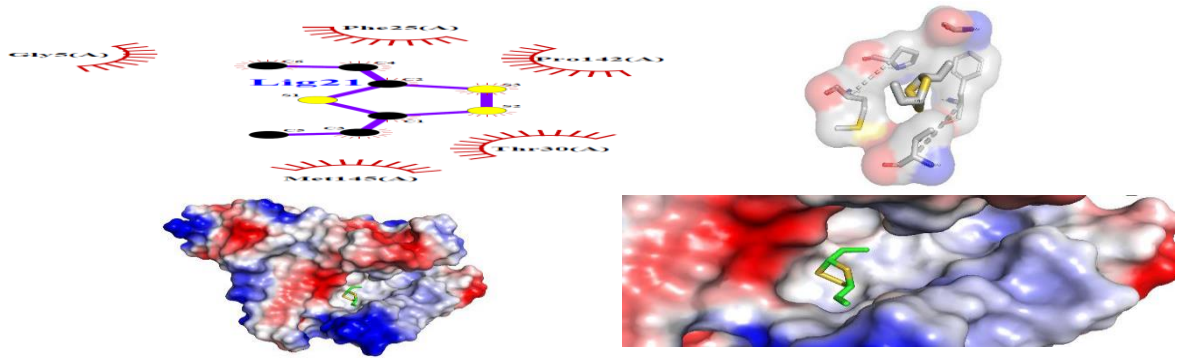

Fig 21 Visualisation of docking interaction and 3D H-bonding, docked pose of lig21

Ligand Code	Binding Affinity (kcal/mol)	No. of H-bonding	H-Bond forming Amino Acids	H-Bond Distance: Donor – Acceptor (A)	Hydrophobic Interaction forming Amino Acids	No. of hydro-phobic bond
Lig21	-4				Gly5(A), Phe25(A), Pro142(A), Thr30(A), Met145(A)	5

CONCLUSION

In the present study 58 compounds were selected from five plants. These compounds were screened using Lipinski's rule of five and determined drug-likelihood of the compound. 21 compounds were drug-likeable which were subjected to molecular docking. Docking results Based on the molecular docking analysis, most of the ligands were showing hydrophobic interaction. Lig18 & lig19 are have greater chance of binding with the modelled target CTXM protein, which is based on the affinity score and interaction. The ligands with greater affinity can thereby have the property to inhibit the CTX-M protein.

REFERENCES

1. Lim, N. M.; Wang, L.; Abel, R.; Mobley, D. L. Sensitivity in Binding Free Energies Due to Protein Reorganization. J. Chem. Theory Comput. 2016, 12, 4620−4631.
2. Gallicchio, E.; Lapelosa, M.; Levy, R. M. Binding Energy Distribution Analysis Method (BEDAM) for Estimation of Protein- Ligand Binding Affinities. J. Chem. Theory Comput. 2010, 6, 2961− 2977.
3. Araki, M.; Kamiya, N.; Sato, M.; Nakatsui, M.; Hirokawa, T.; Okuno, Y. The Effect of Conformational Flexibility on Binding Free Energy Estimation between Kinases and Their Inhibitors. J. Chem. Inf. Model. 2016, 56, 2445−2456.
4. Jones, G.; Willett, P.; Glen, R. C.; Leach, A. R.; Taylor, R. Development and Validation of a Genetic Algorithm for Flexible Docking. J. Mol. Biol. 1997, 267, 727−748.
5. Morris, G. M.; Goodsell, D. S.; Halliday, R. S.; Huey, R.; Hart, W. E.; Belew, R. K.; Olson, A. J. Automated Docking Using a Lamarckian Genetic Algorithm and an Empirical Binding Free Energy Function. J. Comput. Chem. 1998, 19, 1639−1662.
6. Friesner, R. A.; Banks, J. L.; Murphy, R. B.; Halgren, T. A.; Klicic, J. J.; Mainz, D. T.; Repasky, M. P.; Knoll, E. H.; Shelley, M.; Perry, J. K.; Shaw, D. E.; Francis, P.; Shenkin, P. S. Glide: A New Approach for Rapid, Accurate Docking and Scoring. 1. Method and Assessment of Docking Accuracy. J. Med. Chem. 2004, 47, 1739− 1749.
7. L. L.; Pollard, W. T.; Banks, J. L. Glide: A New Approach for Rapid, Accurate Docking and Scoring. 2. Enrichment Factors in Database Screening. J. Med. Chem. 2004, 47, 1750−1759.
8. Friesner, R. A.; Murphy, R. B.; Repasky, M. P.; Frye, L. L.; Greenwood, J. R.; Halgren, T. A.; Sanschagrin, P. C.; Mainz, D. T. Extra Precision Glide: Docking and Scoring Incorporating a Model of Hydrophobic Enclosure for Protein-Ligand Complexes. J. Med. Chem. 2006, 49, 6177−6196.
9. Trott, O.; Olson, A. J. AutoDock Vina: Improving the Speed and Accuracy of Docking with a New Scoring Function, Efficient Optimization, and Multithreading. J. Comput. Chem. 2009, 31, 455−461.
10. Allen, W. J.; Balius, T. E.; Mukherjee, S.; Brozell, S. R.; Moustakas, D. T.; Lang, P. T.; Case, D. A.; Kuntz, I. D.; Rizzo, R. C. DOCK 6: Impact of New Features and Current Docking Performance. J. Comput. Chem. 2015, 36, 1132−1156.
11. Warren, G. L.; Andrews, C. W.; Capelli, A.-M.; Clarke, B.; LaLonde, J.; Lambert, M. H.; Lindvall, M.; Nevins, N.; Semus, S. F.; Senger, S.; Tedesco, G.; Wall, I. D.; Woolven, J. M.; Peishoff, C. E.; Head, M. S. A Critical Assessment of Docking Programs and Scoring Functions. J. Med. Chem. 2006, 49, 5912−5931.
12. Mobley, D. L.; Liu, S.; Lim, N. M.; Wymer, K. L.; Perryman, A. L.; Forli, S.; Deng, N.; Su, J.; Branson, K.; Olson, A. J. Blind Prediction of HIV Integrase Binding from the SAMPL4 Challenge. J. Comput.-Aided Mol. Des. 2014, 28, 327−345.
13. Aldeghi, M.; Heifetz, A.; Bodkin, M. J.; Knapp, S.; Biggin, P. C. Accurate Calculation of the Absolute Free Energy of Binding for Drug Molecules. Chem. Sci. 2016, 7, 207−218.
14. Gaieb, Z.; Parks, C. D.; Chiu, M.; Yang, H.; Shao, C.; Walters, W. P.; Lambert, M. H.; Nevins, N.; Bembenek, S. D.; Ameriks, M. K.; Mirzadegan, T.; Burley, S. K.; Amaro, R. E.; Gilson, M. K. D3R

Grand Challenge 3: Blind Prediction of Protein−Ligand Poses and Affinity Rankings. J. Comput.-Aided Mol. Des. 2019, 33, 1−18.